Methanol Absorption in Ethylene−Vinyl Alcohol Copolymers: Relation between Solvent Diffusion and Changes in Glass Transition Temperature in Glassy Polymeric Materials

Marsha A. Samus and Giuseppe Rossi*

Ford Research Laboratory, Ford Motor Company, P.O. Box 2053, Mail Drop 3083, Dearborn, Michigan 48121-2053

Received June 2, 1995; Revised Manuscript Received November 1, 1995[⊗]

ABSTRACT: The glass transition temperature of a series of ethylene−vinyl alcohol copolymers which have been exposed to methanol is determined by dynamic mechanical measurements as a function of methanol concentration. The results of a number of sorption and desorption measurements taken in the temperature range 21−60 °C for the same polymer−solvent system are also reported. An interpretation of these data, which relates these two sets of results, is presented. This interpretation differs considerably from those currently available in the literature for sorption data similar to those reported here. The need to deconvolute from the sorption data the effect of macroscopic elastic constraints arising during the swelling process and in particular to distinguish features of the sorption curves which reflect true material properties of the system as opposed to simple geometrical effects is pointed out. Once this is done, the main qualitative features of our results, namely, initial sorption $\sim \sqrt{t}$, presence of sharp concentration fronts during sorption, and existence of two different desorption regimes, can be accounted for on the basis of a simple description of solvent transport based on Fick's law with a diffusion coefficient which changes suddenly from a low value characteristic of the glassy state to a high value typical of rubbery polymers at the concentration at which plasticization takes place. The geometry dependent features of the sorption curves can also be understood within this framework.

Introduction

Often the diffusion and uptake of small solvent molecules from a glassy polymer is accompanied by plasticization (*e.g.*, by the undoing of the glassy state). In order to correctly describe this type of process, it is useful to have a simple picture of the motion of solvent molecules within the polymer at the microscopic level. The microscopic processes which influence the diffusion of small molecules in the glassy and plasticized regions are clearly different.

For polymeric material in the glassy state, all but the most local movements of the polymer molecules are inhibited. Portions of chains containing more than a few monomers are unable to move with respect to each other, and those motions of single monomeric segments which are not impeded are constrained to microscopic regions whose size is comparable to the monomer size.[1] Unless the monomeric structure is such to entail the existence of empty regions between chain segments large enough (in comparison to a permeant molecule size) to provide a network of routes for the permeant across the material,[2] the movements of small molecules within a glassy polymer are very severely hindered.

On the other hand, when viewed on a molecular scale, the amorphous regions in rubbery (plasticized) polymeric material behave like a (polymeric) liquid: Movements of relatively large portions of the chains with respect to each other are possible, and in the course of these movements, formation and displacement of voids sufficiently large to accommodate permeant molecules do take place. As a result, it is relatively easy for a permeant molecule to move through such a material. The large differences (often by orders of magnitude) between the values of the diffusion coefficients of the same permeant in glassy and rubbery polymers[3,4] can be qualitatively rationalized on the basis of these ideas.

A considerable amount of experimental results regarding solvent diffusion in glassy polymers has accumulated over the years. In many instances, the final solvent uptake is very small[3,5,6] and is not sufficient to induce plasticization, so that the polymeric material remains glassy even after the solvent concentration within the polymer-occupied region has become uniform.[7] In these instances, it is generally agreed that the diffusion process is Fickian, *e.g.*, that the flux is proportional to the local gradient of the concentration, and that it can be described using a diffusion coefficient, $D(T)$, dependent on temperature.[8] In fact, the discontinuity in the slope of $D(T)$ (change in activation energy) observed at $T = T_g$ in the systems of ref 5 points to the difference between the microscopic mechanisms responsible for the diffusion of small molecules in glassy vs plasticized material.

In situations where plasticization takes place, a variety of different behaviors have been reported. In several systems[9−16] initial uptake linear in time together with sharp fronts which move at constant velocity and separate the glassy and plasticized portions of the specimen have been observed. This behavior is ordinarily referred to as case II diffusion. In a number of such systems the velocity of front advancement has been observed to slow down at later times.[11,12] Furthermore, when the temperature of the experiment approaches the glass transition temperature, T_g, of the polymer, both the distance covered by the plasticization front and the solvent uptake have been reported to increase as t^α (with α intermediate between 0.5 and 1) even at short times.[11−13] Plasticization can also occur in systems[10,17−22] where the initial ($t \rightarrow 0$) solvent uptake grows like $\sqrt{t}$. In a number of such instances,[10,22] sharp fronts which move at velocity $v \sim t^{-1/2}$ and separate the glassy from the plasticized portions of the specimen have been observed.

A variety of experimental techniques have been applied to the study of solvent diffusion in glassy

[⊗] Abstract published in *Advance ACS Abstracts,* February 15, 1996.

0024-9297/96/2229-2275$12.00/0

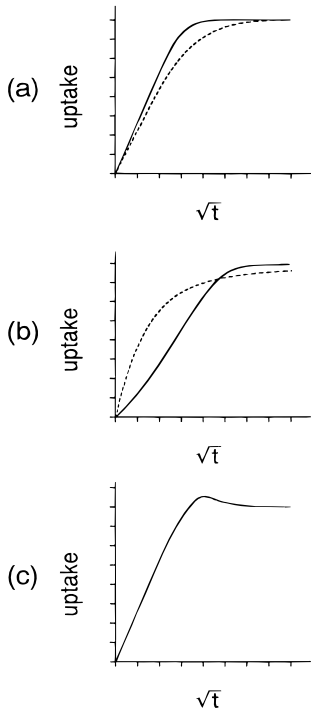

Figure 1. (a) Sorption (continuous line) and desorption (broken line) curves obtained solving the ordinary diffusion equation in one dimension with a diffusion coefficient, $D(c)$, which increases with solvent concentration. (b) Sorption (continuous line) and desorption (broken line) curves displaying features which have been ordinarily described as "anomalous" or "non-Fickian". These include "sigmoidal" sorption (following the inflexion point there is a regime of accelerated uptake), initial desorption faster than sorption, and desorption curve crossing the sorption curve at finite times. (c) Sorption curve displaying an "overshoot" before equilibrium is achieved.

polymers.[23] Concentration profiles can be obtained with varying degrees of spatial resolution using such methods as microdensitometry,[13,24,25] Rutherford backscattering,[14,15,26] and forward recoil[16] spectrometry. However the bulk of available data regarding these systems comes from sorption (and desorption) experiments, where the weight gain (or loss) of polymer exposed to a certain solvent activity is tracked as a function of time. Sorption data have also been complemented by measurements of the change in the physical dimensions of the specimen as a function of time.

In the past, there has been a tendency[27] to describe as "anomalous" or "non-Fickian" any deviation of the shape of the observed sorption curves from the shape which is obtained solving the ordinary diffusion equation in one dimension with boundary conditions which imply that the surface equilibrium is established as soon as the polymer is exposed to the diffusant (see Figure 1a). Features which have been usually described as "non-Fickian" include an inflection point in the sorption curves at finite time resulting in the so-called "sigmoidal" (or "S") shape (see Figure 1b) and desorption taking place faster than sorption (see figure 1b), as well as sorption "overshoots", *e.g.*, the observation at intermediate times of uptake larger than the final equilibrium uptake (see Figure 1c). Furthermore, since the great majority of experimental work is carried out with films or slab-shaped samples (where the thickness is much smaller than the width or the length), it has often been assumed that a one-dimensional description of the processes occurring as diffusant penetrates the polymer is appropriate.

In order to correctly interpret sorption data, it is essential to realize that a weight gain curve represents the integral at a given instant of time of the concentration of solvent within the sample. As such the shape of the sorption curve at finite times depends strongly on the physical shape and geometry of the sample: It is a kind of average of the various physical processes which may be taking place,[28] and it is not necessarily a good indicator of which microscopic processes are actually occurring. As an example of this, we note that the apparently "anomalous" sorption and desorption curves of Figure 1b were in fact obtained from equations[29,30] which describe diffusion of a solvent into a cross-linked polymer sphere and are based solely on Fick's law with the standard boundary conditions, *e.g.*, on precisely the same assumptions used to generate the curves of Figure 1a; even the concentration dependence ($D(c) \sim e^{\alpha c}$, with $\alpha = 6$) of the diffusion coefficient is the same. The difference between the two figures is that in Figure 1b we consider a spherical geometry and furthermore that we account for the swelling of the polymer as solvent moves in.[31]

The interpretation of sorption data is further complicated by the fact that a pronounced "sigmoidal" shape may result in a portion of the weight uptake vs time plot displaying apparent linearity in time[32] at finite times. Furthermore, even more complex sorption curves (two-stage behavior) can be obtained if Fick's law is valid, but the request that equilibrium be attained instantaneously at the sample surface is relaxed.[33] In view of all this, it seems fair to conclude that little unequivocal indication of "non-Fickian" behavior can be gleaned from the sorption curves, unless the initial ($t \rightarrow 0$) uptake is not proportional to $\sqrt{t}$. The $t \rightarrow 0$ limit should reflect true material properties of the solvent−polymer pair: At $t \rightarrow 0$, any geometry is effectively semi-infinite; only the surface layer is affected, and the large scale geometry of the sample should be unimportant.

As solvent moves into the glassy polymer and the polymer becomes plasticized, it swells, typically by an amount nearly equal to the volume of the solvent taken up. In fact, during plasticization changes in free volume will also take place, but they should amount to only a small fraction of the total volume increase. In order to correctly capture the physics of this process and in particular to obtain estimates of the kind of elastic forces which develop between regions of the sample swollen to a different extent, it is crucial to realize that the swelling process is inherently three-dimensional.[34]

Some time ago, Treloar[35] treated the problem of the equilibrium swelling of a cylindrical rubber tube whose inner surface is adhesively bonded to a rigid (*e.g.*, metal) cylindrical core. The analog spherical geometry (a spherical polymer shell bonded to a rigid sphere) has also been investigated.[36] These problems are especially relevant to diffusion of solvent into a glassy polymer when a sharp front separating the glassy from the plasticized region is present. This is because the modulus of the glassy core can be orders of magnitude higher than the modulus of the plasticized region and effectively behaves as the rigid core[9] in Treloar's problem.

Since Treloar deals with the equilibrium rather than the kinetics problem, Treloar's results for a given quantity should be regarded as upper or lower limits on the value taken by that quantity during the diffusion process. For example, consider the initial stages of solvent penetration into a glassy polymer film. The

appropriate analogous constrained swelling problem is that of a thin spherical rubber shell bonded to a rigid spherical core whose radius tends to infinity. Therefore, the solvent volume fraction in the plasticized region close to the surface of the film will be at most equal to the value predicted by Treloar's calculation for the thin spherical shell.[37] Initially (limit of vanishing shell thickness) the tensile force perpendicular to the surface of the film is zero, while the plasticized region is subject to compressive forces parallel to its surface (correspondingly the core experiences tensile forces parallel to the surface[38]).

In the equilibrium Treloar's problems for the cylinder or the sphere, as the thickness of the rubber layer increases tensile forces perpendicular to the surface develop (these forces are largest at the interface), while the compressive forces parallel to the surface decrease in magnitude. Within the rubber layer there is a solvent concentration gradient; the concentration is lowest close to the rigid core: At the outer surface it is lower than it would be in the absence of the core. Similarly, in the process of solvent diffusion into cylindrical or spherical samples, as the glassy−plasticized interface moves away from the surface, tensile forces perpendicular to the surface will develop, and their magnitude will be smaller than those obtained from the corresponding Treloar problem since the solvent concentration is lower than in the equilibrium case. In a film, where apart from edge effects the curvature of the rigid layer is zero, the tensile forces perpendicular to the surface will be negligible, throughout the kinetic process. Note that, independently of the thickness of the rubber layer, the spherical Treloar problem in the limit of infinite core radius (to which the film situation corresponds) has no concentration gradient: The magnitude of the compressive stresses parallel to the core surface is independent of the thickness of the rubber layer.

In contrast to these results, in a strictly one-dimensional version of the Treloar problem, *no* elastic forces arise; the solvent concentration is uniform throughout the rubber layer, and its value is the same as that found in an unconstrained sample.[39] These results point to the inadequacy of a purely one-dimensional description of the stresses accompanying the swelling process in polymeric materials where, in the course of solvent diffusion, different regions of the specimen exhibit large differences in moduli.[40]

In light of these considerations, let us now consider uptake of solvent into a glassy polymer slab in a situation where a sharp front separates the glassy from the plasticized region. Initially, the plasticized layer can swell only in the direction perpendicular to the film surface. The rigid inner region prevents swelling in the other two directions and limits the concentration of solvent at the surface to a level lower than the final equilibrium concentration (see Figure 2b). The constraint from the rigid core is released when the solvent reaches the central region of the film and the material in this region becomes plasticized. Only at this point can the polymer swell in the other two directions (see Figure 2c), and the value of the solvent concentration grows to the final equilibrium value. We believe that this simple mechanism (which has been described before in the context of swelling of polyelectrolyte gels[41−43]) is at the origin of the regime of accelerated uptake (leading to "sigmoidal" sorption curves) which is often seen in glassy polymer films. We expect the onset of the accelerated regime to coincide with a dramatic change in the transverse dimensions (length and width) of the film. Furthermore, if the initial uptake (prior to the onset of the accelerated regime) is Fickian, the time at which the onset of the accelerated regime occurs should scale with l^2, where l is the thickness of the film.

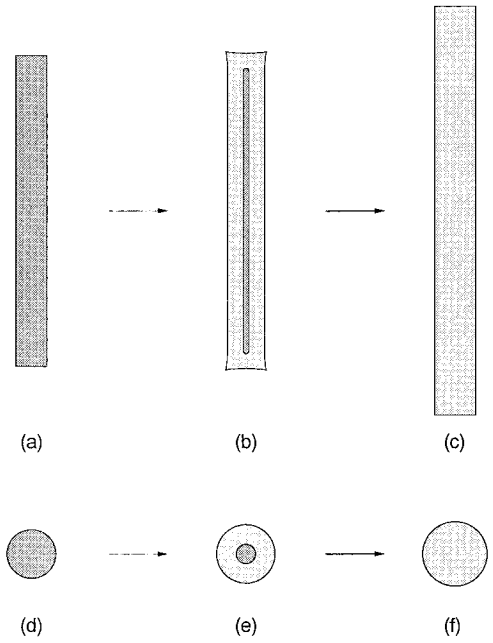

Figure 2. Diagram of film or slab. In a swelling film or slab (a), *i.e.*, when one of the dimensions of the sample is much smaller than the others, swelling can take place only in the direction perpendicular to the face of the film as long as the central region of the film remains glassy (b). When eventually the central region becomes plasticized, the sample swells in the other directions (c) resulting in a regime of accelerated uptake. On the other hand, in a swelling sphere (d), swelling is isotropic from the beginning (even though elastic stresses between the inner core and the plasticized region are still present) so that constraint release is gradual (e and f) and does not suddenly change at some finite time.

If the shape of the specimen is different from that of a film or a slab, we expect the shape of the sorption curves to be different. In particular, for a cylindrical sample, swelling is initially prevented only in the direction of the axis of the cylinder, so we expect accelerated uptake to play a lesser role than in the case of the films. For spherical samples (see Figure 2d−f), where swelling can take place isotropically from the start, constraint release is gradual, and there should be no dramatic signature of accelerated uptake in the sorption curves.

Clearly, processes of the kind just described play a role even in the absence of a sharp concentration front between the glassy and plasticized region, as is, for example, the case in differential sorption experiments, where the solvent activity to which the sample is exposed is changed in small steps and at each step the sample is allowed to come to equilibrium. The elastic moduli of a given region of the sample depend on the local concentration of solvent, and if differences in local concentration between different sample regions are small, a "smoothed" version of the mechanism described above will be at work. We note in this regard that it is sometimes claimed[44] that differential sorption experiments are "unambiguous" on the grounds that within each step there should be little change in the elastic moduli and the diffusion coefficient. However, the fact is that there is no obvious way to deconvolute from the

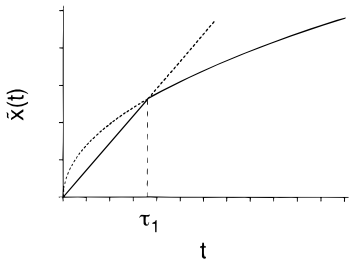

Figure 3. Competing effect on the distance $\tilde{x}(t)$ covered by the front of the plasticization kinetics (straight line) and solvent transport (square root). The slowest of the two mechanisms limits the movement of the front. The plasticization kinetics control the slope of the straight line: If it is fast, Fick's law controls the movement of the front from the very beginning (*e.g.*, τ_1 is very small), otherwise a long case II regime is predicted.

sorption results the constraint release effects described above. Furthermore, around the solvent concentration at which plasticization occurs, both the moduli and the diffusion coefficient can change very rapidly even within a small concentration interval.

If sorption experiments are carried out just above the nominal T_g, the elastic moduli can still experience significant changes as the concentration of solvent within the sample increases (for an example, see Figure 4). Again the kind of mechanism described above will be active. It may have an effect in some of the "anomalies" reported for a number of systems under such conditions.[45]

A brief review of recent attempts to deal with solvent diffusion in glassy polymers is now in order. A critical review of models and theories put forward up to the late 1970's can be found in the first of ref 7, and we shall not cover those models here.

A phenomenological model which provides a rationale for the observed case II behavior was proposed in 1978 by Astarita and Sarti.[46] The physics of the Astarita–Sarti model is simple and can be rephrased as follows:[47] Two different physical processes (solvent transport and plasticization[48]) take place as solvent moves into the sample. Solvent transport occurs only in the plasticized region where it is described by Fick's law with a diffusion coefficient, D_1 (in the glassy region the diffusion coefficient is zero[49]). Plasticization can only take place if the volume fraction of solvent exceeds a certain value, $\tilde{\phi}$, and the kinetics of the transition from the glassy to the rubbery state set an upper limit for the velocity, v, of the plasticization front. Should there be no such upper limit, the location, $\tilde{x}(t)$, of the front (*e.g.*, the point where the solvent volume fraction equals $\tilde{\phi}$) would simply move according to Fick's law, $\tilde{x}(t) \sim (D_1 t)^{1/2}$. However, if v sets an upper limit for the front velocity, the front will move according to $\tilde{x}(t) = vt$, up to time $\tau_1 \approx D_1/v^2$; for $t > \tau_1$, the movement of the front becomes transport limited. This behavior is illustrated in Figure 3. If v is small, case II behavior will persist up to very large times. On the other hand, if v is large, the kinetics of plasticization play a role only for a very short time, and solvent uptake is for all practical purposes controlled by Fick's law. Other experimental features, such as the existence of an induction time preceding the establishment of a moving plasticization front, can be predicted within this framework if the initial ($t \rightarrow 0$) regime is dealt with consistently.[47]

A considerable amount of effort has been devoted to the problem of relating the velocity of front advance in case II diffusion to other material properties. Sarti[50] tried to establish a connection with the phenomenon of craze formation. Thomas and Windle[51] invoked a viscous resistance to swelling with a local viscosity exponentially dependent on concentration: The parameters in this model can be chosen in such a way that a number of experimental features are reproduced.[14,15]

A number of authors[52−56] have attempted to relate "non-Fickian" or "anomalous" features in the sorption curve to a Deborah number which is defined as the ratio of a characteristic relaxation time, τ_R, for the material and a characteristic diffusion time, τ_D, which is taken to be proportional to the square of the sample thickness, $\tau_D \sim L^2$. According to these authors "non-Fickian" sorption is to be expected when the order of magnitude of $\tau_R/\tau_D \approx 1$, while Fickian behavior should be found when τ_R/τ_D is either much larger or much smaller than 1. The following criticism can be raised regarding these ideas. They imply that a system such as PMMA in MeOH, which for samples with $L \approx 1$ mm exhibits case II behavior at room temperature, will exhibit Fickian behavior if a sufficiently thick slab of PMMA is used; presumably, the fronts would either disappear altogether or at least start moving with velocity $\sim t^{-1/2}$ at $t \rightarrow 0$, simply because the slab of PMMA is now thick (note that even for a PMMA slab ≈1 mm thick about 1 week is required for the two fronts to meet). Likewise, systems such as natural rubber or polyethylene in toluene, which display Fickian behavior for film thicknesses of the order of 1 mm, should according to these ideas begin to display "non-Fickian" (or perhaps case II) behavior if sufficiently thin films are used. These implications are paradoxical and unphysical.[57] They cast serious doubts on the soundness of these ideas[58] and on their relevance to the problem of solvent diffusion in polymeric materials.[59]

It should be noted that no such paradox arises within the context of refs 46 and 47. The parameter τ_1 (whose size determines the transition from linear to $\sqrt{t}$ behavior) is the ratio of two quantities (D_1 and v^2), *both* of which are material properties independent of the size of the sample. At $t \rightarrow 0$, the advancing methanol fronts move at a constant velocity no matter what the value of L is. A crossover to velocity $\sim t^{-1/2}$ is predicted for $L > v\tau_1$, but this in no way implies a change in the basic physics of the process.

The models criticized above seek to account for the "non-Fickian" features of the sorption curves by using constitutive relations for the local flux different from Fick's law.[60] The new relations are assumed to hold throughout the sample and usually entail one or more (often vaguely defined) relaxation times.[61] However, if one considers a system where a sharp front is present, say one undergoing case II diffusion, it appears that the only obvious "violation" of Fick's law takes place at the front, where a different phenomenon (plasticization) is occurring anyway.[62] It seems to us that when the kinetics of plasticization are properly taken into account, for example, by imposing an upper limit on the flux into the glassy material,[47] there may be no need to invoke some fundamental violation of Fick's law. Indeed, the situation may be similar to that of systems where in addition to diffusion chemical reactions occur; the sorption curves and the concentration profiles may look odd, but this is a consequence of the fact that in addition to diffusion the chemistry of the material is changing. In this paper we explore the extent to which the constraint release mechanism (which accompanies plasticization) can account for some of the odd features

which have been customarily described as "non-Fickian". Some may argue that such a mechanism is a "non-Fickian" feature. However, an obvious analog is that of a rubber which swells while constrained by some mechanical device until at some point the constraint is suddenly released. It is clearly inappropriate to describe such an event as a "non-Fickian" process, let alone to invoke some fundamental modification of Fick's law to account for it.

We conclude this brief review noting that while a number of other models can be found in the literature,[63] the status of our present understanding of the subject of solvent diffusion in glassy polymers is probably best summarized by the fact that there seems to be no reliable self-consistent framework within which such quantities as solvent uptake and loss and solvent concentration profiles as a function of time can be quantitatively predicted.

In this paper we consider a system for which the initial uptake is $\sim\sqrt{t}$ (within the temperature range that we examine): Our polymer−solvent pair is a random copolymer of ethylene and vinyl alcohol (EVOH) in the presence of methanol. First we examine the dependence of the dynamic mechanical spectrum and in particular of the glass transition temperature, T_g, on methanol concentration. These results provide information on the level of methanol which induces plasticization at a given temperature and on the change in the elastic moduli of the system as a function of methanol concentration. Next the results of a number of sorption (in liquid methanol) and desorption measurements in the temperature range 21−60 °C are presented. We discuss and interpret these results on the basis of the simple qualitative ideas put forward in the first part of this section. In particular, we present evidence indicating that the regime of accelerated uptake observed in the sorption curves for slab-shaped samples can be understood in terms of the constraint release effects discussed above. We find that in order to interpret the experimental results correctly, it is essential to distinguish between results which are due to microscopic (material) properties of the system and results which are due to the particular geometry of the sample, *e.g.*, to the rise and eventual release of macroscopic elastic stresses between the glassy and plasticized portions of the specimen. In the system that we study, the first class of results can be consistently rationalized in terms of a simple physical picture whose central ingredient is Fickian diffusion with a diffusion coefficient which changes drastically at the plasticization concentration in accordance with the ideas outlined at the very beginning of this section. Furthermore, within this framework, it is possible to quantify the effect of the geometry dependent results on the sorption curves, using the constraint release mechanism discussed above.

This paper is organized as follows. In the next section we describe our experimental setup and present the results of our dynamic mechanical study and our sorption and desorption experiments. The last section contains our interpretation of these results and a discussion of their significance in relation to the general problem of solvent transport in glassy polymers.

Experimental Section

Commercial EVAL (ethylene vinyl alcohol) random copolymer resins were obtained from Evalca-Kuraray for use in this study. In all the sorption and desorption measurements reported here, EVAL-F101 was used. F101 has an ethylene copolymer ratio of 0.32, a melting point (by DSC) of 183 °C, a density of 1.19, a molecular weight of 41 400, and a polydispersity index $M_w/M_n = 2.2$, as specified by the supplier. In the dynamic mechanical study, in addition to F101, two other resins were used, L101A with a ratio of 0.27 and melting point of 191 °C and G110 with a ratio of 0.44 and melting point of 158 °C. Sample plaques of these materials were compression molded in 1.2 mm window molds under 16 tons of pressure at 220 °C for L101A and at 200 °C for F101 and G110. Molds were cooled under pressure in a cold press for 30 s, except for one set of samples of F101, designated F101s, which was slowly cooled to room temperature over the course of 16 h.

All specimens used for dynamic mechanical evaluation required further preparation to increase dimensional uniformity. Specimens of *ca.* 0.7 mm thickness, 12.4 mm width, and 65 mm length were prepared from the compression-molded EVOH plaques by careful sanding, to minimize frictional heating and preserve the thermal history of the samples. Thickness variations along the length of the samples were held to within 0.02 mm. These specimens were held under vacuum for at least 18 h at 40 °C and then stored over dessicant until use. Dynamic mechanical spectra were obtained in shear for "neat" and solvent-soaked specimens on a Rheometrics RMS-800 mechanical spectrometer in torsion rectangular geometry. Isochronal spectra were obtained from either −70 or −50 to 100 °C at 0.2% strain (verified to be within the linear viscoelastic region), 240 g tension, and a frequency of 1 Hz.

Specimens used to quantify solvent effects on the glass transition temperature were soaked for varying lengths of time in methanol, in sealed vials. In this way different levels of solvent uptake within the specimens were obtained. After soaking, all samples (except those that had been kept in solvent for more than 3 months) were sealed in clean vials. They were held there for a time that we deemed sufficient to ensure equilibration of concentration gradients within the sample.

Dynamic mechanical spectra were taken only after this equilibration procedure. For specimens held in solvent for more than 3 months, spectra were taken immediately following soaking on the assumption that equilibrium at the measured level of solvent uptake had been reached at that point. In a number of instances, further intermediate solvent concentrations were obtained by placing soaked specimens under vacuum for a short time at 100 °C and then allowing them to re-equilibrate.

Sorption and desorption measurements were made using either molded specimens sanded to the desired thickness or extruded films obtained from Evalca-Kuraray. In all the film and slab specimens, the thickness was at least 1 order of magnitude smaller than the other two dimensions. Prior to sorption the specimens were annealed in vacuum at 100 °C for at least 2 days. Sorption specimens were held in liquid methanol (contained in a round-bottomed flask equipped with a reflux condenser) and kept at a constant temperature (±1 °C). Specimens were removed periodically from the methanol bath, wrapped in aluminum foil, and weighed before being unwrapped and returned to the solvent. Data were corrected for out of bath time, and no significant desorption occurred during weighing of sorption specimens. Specimens which had been held in liquid solvent for a time sufficiently long to reach equilibrium were desorbed in a vacuum oven at constant temperature. Again weight measurements of these desorbing samples were taken periodically.

Effect of Methanol on T_g. Dynamic mechanical spectra of EVAL-F101 specimens are shown in Figure 4 for different levels of methanol uptake. The figure shows both the shear storage modulus, G', and the ratio $\tan\delta = G''/G'$ between loss and storage moduli as a function of temperature.[64] The glass transition temperature of the specimen (maximum in $\tan\delta$) moves to lower and lower values of T as the methanol concentration increases. Even though T_g changes, the low-temperature value of G' in the glassy state at low methanol levels is nearly unchanged by the presence of solvent. The two distinct maxima in $\tan\delta$ (one at ≈−25 °C and one at ≈68 °C) found in the dry copolymer merge in the presence of MeOH into one intermediate transition, and the $\tan\delta$ minimum at

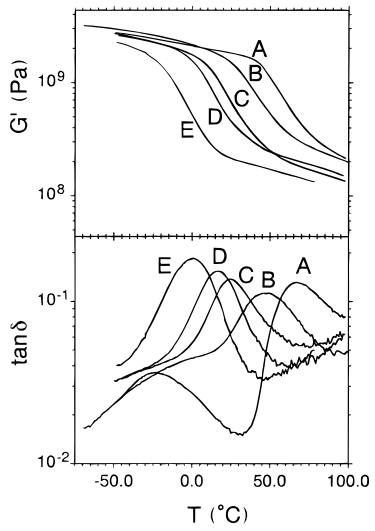

Figure 4. Dynamic mechanical spectra for EVOH-F101 at different levels of MeOH uptake. The upper part of the figure shows the storage moduli, G', vs T, and the lower part shows the loss tangents, tan δ. The methanol weight fraction in the sample before the run (weight of absorbed methanol as a fraction of total sample weight) was 0.0 (A), 0.022 (B), 0.031 (C), 0.053 (D), and 0.084 (E).

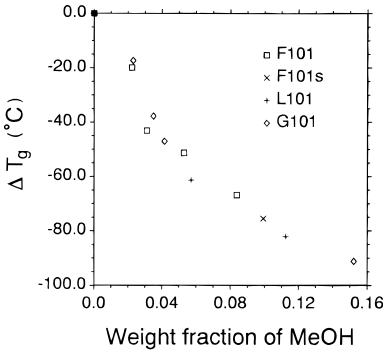

Figure 5. Downward shifts in the glass transition temperature, T_g (maximum in tan δ), for EVOH in the presence of methanol as a function of the methanol weight fraction in the sample (weight of absorbed methanol as a fraction of total sample weight).

≈30 °C disappears. This suggests a strong structural coupling between the motions responsible for the transitions. This merging also indicates that no large concentration gradient exists in the equilibrated specimens.

These results show that MeOH does act as a plasticizer for the copolymers. Indeed, the shifts in T_g and the results for the shear storage moduli, G', in the presence of methanol are very similar to dynamic mechanical results reported in the literature[65] for poly(vinyl alcohol) in the presence of glycerol (a standard plasticizer for PVA). Results similar to these were obtained for the F101s, L101A, and G110 samples: In these instances the maximum in tan δ for the dry materials is found at $T \approx 65$, 72, and 57 °C, respectively.

Figure 5 summarizes the correlation between drops in glass transition temperature and methanol uptakes for all of our EVOH specimen. Although the T_g's of the different dry EVOH materials differ by ≈15 °C, the dependence of the T_g drop on solvent concentration is essentially the same. At low levels of methanol, T_g is lowered about 10 °C for each weight percent methanol uptake. Again these results are similar to those reported in ref 65 for water or glycerol in poly(vinyl alcohol) and consistent with data for other polymer−solvent systems reported in the literature.[1,7,18]

Sorption and Desorption Results. Examples of our sorption curves for EVOH slabs immersed in liquid methanol at different temperatures are shown in Figure 6. The figure gives the fractional weight uptake of methanol, namely, $(w_t - w_i)/(w_f - w_i)$, where w_t, w_i, and w_f are respectively the weight at time t, the initial weight, and the final weight of the sample, in F101s as a function of $\sqrt{t}/l$, where l is the thickness of the slab. The curves of Figure 6 refer to 29 (●), 40 (□), and 59 (○) °C. The final equilibrium amount of methanol, $c_{eq} = (w_f - w_i)/w_f$, *e.g.*, the final weight of absorbed methanol as a fraction of final total weight, is $c_{eq} = 0.104$ at 29 °C, 0.112 at 40 °C, and 0.148 at 59 °C. No significant solvent loss (*e.g.*, "overshoot") was observed after the maximum uptake was reached.[66]

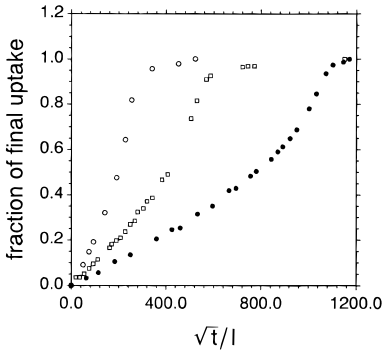

Figure 6. Fractional weight uptake of methanol in F101s as a function of $\sqrt{t}/l$, where l is the thickness of the slab in millimeters and t is time in seconds. These data were taken at 29 (●), 40 (□), and 59 (○) °C.

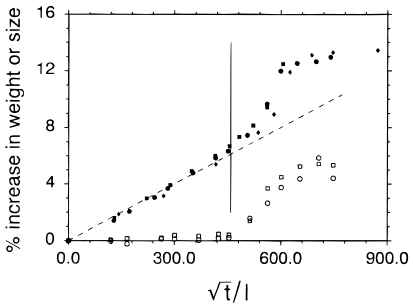

Figure 7. Percent weight increase obtained at 40 °C for three films of thickness 77 (♦), 140 (■) and 225 (●) μm plotted as a function of $\sqrt{t}/l$, where l is the thickness of the film in millimeters and t is time in seconds. Percent width (○) and length (□) increase for a 225 μm film undergoing sorption at the same temperature are also displayed. The continuous vertical straight line marks the onset of the regime of accelerated uptake (identified by the departure of the sorption points from the initial $\sim\sqrt{t}$ behavior denoted by the dashed line) and coincides with the beginning of a drastic change in the trasverse dimensions of the sample.

Our sorption curves exhibit sigmoidal shape similar to that reported in the past for a number of other solvent−glassy polymer systems.[17−22] Initially the weight uptake grows like $\sqrt{t}$, but at later times a region of accelerated uptake is observed. We attribute this behavior to macroscopic elastic constraints being exerted by the as yet unswollen central region of the specimen on the outer plasticized regions while the diffusion process takes place. When the central portion of the slab is plasticized, this constraint is released, leading to the observed accelerated uptake. As we discussed in the Introduction, if this interpretation is correct we expect the onset of the regime of accelerated uptake to coincide with a sudden increase in the transverse dimensions of the film.[67] Furthermore, if Fickian diffusion controls the initial swelling process, we expect the onset of the acclerated regime to coincide for films of different thickness when the weight uptake is plotted against $\sqrt{t}/l$. An example, which shows how both expectations are met in our system, is given in Figure 7. The percent weight increase (*i.e.*, $100 \times (w_t - w_i)/w_i$) obtained at 40 °C for three films of thickness (77, 140, and 225 μm) is displayed together with the percent increase in sample width and length for a 225 μm sample. The sorption results are clearly superposable (within experimental error) when plotted

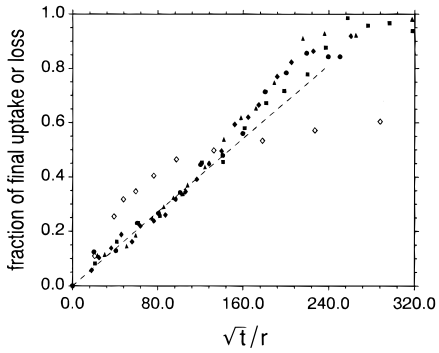

Figure 8. Fractional weight uptake (filled symbols) as a function of $\sqrt{t}/r$ for four small cylindrical specimens of radii ≈0.69 ± 0.02 (●), ≈0.62 ± 0.01 mm (♦), ≈0.47 ± 0.01 (▲), and ≈0.40 ± 0.01 (■) mm. These data were taken at 50 °C. The sample length is ≈3 cm, and $c_{eq} = 0.167$. The departure of the sorption data from the dashed line marks the onset of accelerated uptake. A set of desorption data at 50 °C for the cylinder of radius ≈0.47 (◊) is also shown.

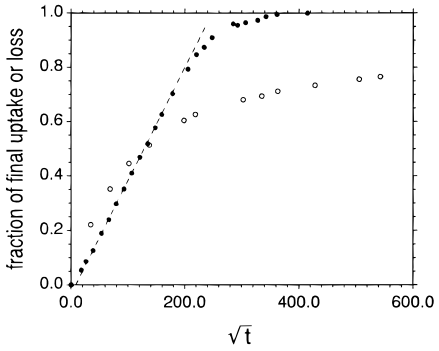

Figure 9. Fractional weight uptake at $T = 60$ °C (●) and loss at $T = 55$ °C (○) of methanol from a set of five small (nearly) spherical pellets of F101 as a function of $\sqrt{t}$, where t is time in seconds ($c_{eq} = 0.178$, diameter = 3.00 ± 0.04 mm).

vs $\sqrt{t}/l$. The onset of accelerated uptake, identified by the departure from the original $\sqrt{t}$ behavior (dashed line in the figure), does coincide with the onset of a drastic change in the transverse dimensions of the sample.

In order to obtain some information on the shape of the concentration profiles, we performed a few sorption experiments using methanol tinted with iodine.[13] By sectioning the EVOH specimens at intermediate times during sorption, sharp fronts separating a white (presumably dry) core from the outer colored regions can be observed under an optical microscope. We did not attempt to measure the front velocity[68] nor to perform a microdensitometric analysis of the kind described in ref 13.

We performed a number of sorption experiments with cylindrical and spherical samples. As noted in the Introduction, in these samples macroscopic elastic constraints should arise and be released in ways different from the way in which they manifest themselves in films or slabs. As a result, the shape of the sorption curves at finite times should also be different. Examples of our data are given in Figures 8 and 9. Figure 8 shows sorption results for four small cylindrical specimens whose radius ranges between ≈0.40 and ≈0.69 mm (the length is ≈3 cm) taken at $T = 50$ °C. In these data the initial ($t \rightarrow 0$) uptake is consistent with $\sqrt{t}$ growth (dashed line): The data from the different samples superpose when plotted against $\sqrt{t}/r$. At later times there is a regime of accelerated uptake; however, the effect is considerably smaller than in the case of the films. Figure 8 also shows a set of desorption data at 50 °C.

Figure 9 shows both sorption (at $T = 60$ °C) and desorption (at $T = 55$ °C) data for a set of five small spherical pellets of F101. In this case there is no accelerated uptake late in the sorption process. Again the sorption data at small t fall on a

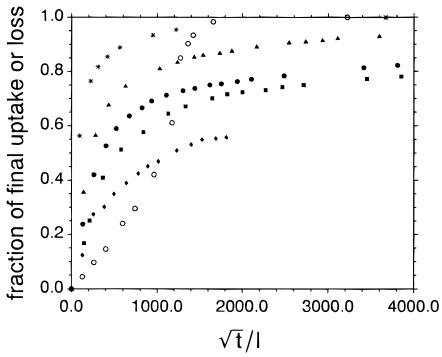

Figure 10. Desorption data for F101 films. After having been equilibrated in MeOH at room temperature ($c_{eq} = 0.121$), they were left to desorb in vacuum at various temperatures: 21 (♦), 32 (■), 40 (●), 55 (▲), and 90 (*) °C. For comparison, a set (○) of sorption data (taken at 25 °C) from one of these films is also shown. The fractional weight uptake and loss are plotted against $\sqrt{t}/l$, where l is the thickness of the film in millimeters and t the time in seconds.

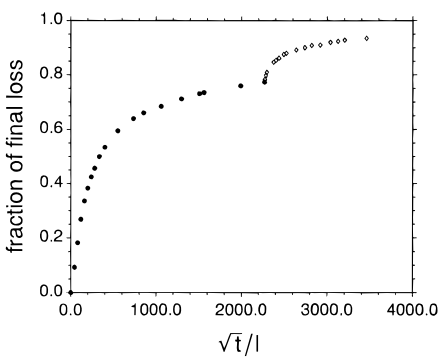

Figure 11. Desorption curve for an F101 slab. After having been equilibrated in MeOH at $T \approx 55$ °C ($c_{eq} = 0.178$), it was left to desorb in vacuum at 23 °C (●); eventually the temperature was raised to 50 °C (◊). The fractional weight loss is plotted against $\sqrt{t}/l$, where l is the thickness of the slab in millimeters (here $l = 380$ μm) and t is the time in seconds.

straight line when plotted against $\sqrt{t}$ (see dashed line in the figure). However, this line does not go through the origin. The effect is small (the intercept of the line on the time axis is found at $t \approx 60$ s) but reproducible, and it is not obvious that it should simply be dismissed as an experimental artifact. Since we found initial $\sqrt{t}$ uptake in both films and cylinders at lower temperatures, this behavior cannot be attributed to our system belonging (like the system of ref 13 at high T) to the crossover range between case II and Fickian regimes predicted by the models of refs 46 and 47: If this was the case we should have uncovered similar but more noticeable effects in the data collected at lower temperatures.

Examples of our desorption data are shown in Figure 10. These data were taken at different temperatures (♦, 21 °C; ■, 32 °C; ●, 40 °C; ▲, 55 °C; *, 90 °C) for film samples which had all been soaked at room temperature. The desorption process is initially faster than sorption at the same temperature; a set of sorption data for one of these films (○) at 25 °C is shown in the figure for comparison. At later times a regime where loss occurs extremely slowly is reached for all samples except the one where desorption was carried out at 90 °C, *e.g.*, above T_g. The solvent level at which this "slow-desorption" regime occurs depends on the temperature of the experiment. Note that a similar "slow-desorption" regime is found for both cylinders (Figure 8) and spheres (Figure 9). If the temperature is increased once the "slow-desorption" regime is reached, there is a brief period of fast desorption before a new "slow-desorption" corresponding to the new temperature sets in. An example of this effect is shown in the curve of Figure 11: In this case desorption began at room temperature (●), but T was later raised to 50 °C (◊).

Discussion

The data presented in the previous section underscore the need of distinguishing between experimental results which reflect true material (microscopic) properties of the polymer−solvent system and results which depend on the geometry and size of the sample. In this section we pursue such an analysis by first isolating those features which belong to the first class and setting up a simple framework which accounts for them. This framework emphasizes the interplay between diffusion and changes in the glass transition temperature of the material as solvent penetrates it. In the second part of this section we present the results of a number of simple calculations which permit us to rationalize the geometry dependent features of the sorption and desorption curves in terms of the constraint release mechanism discussed in the Introduction. Again the glass transition plays a crucial role in these arguments.

Three main qualitative features stand out from the experiments described in the previous section as independent of sample geometry and characteristic of the process of MeOH diffusion in EVOH. These are (i) uptake which initially grows like $\sqrt{t}$, (ii) presence of a sharp front between the glassy and plasticized portions of the specimen during sorption, and (iii) existence of two regimes for desorption: an initial fast regime followed by a very slow desorption regime whose onset depends on the temperature of the experiment. A fourth feature which appears to be common to all samples is the fact that desorption is initially faster than sorption. We shall see later that this result has a simple explanation in terms of constraint release. Therefore, we begin our analysis by trying to account for the three features listed above.

It should be clear, from the qualitative picture put forward at the beginning of this paper and the difference between measured values of the diffusion coefficient for the same penetrant in glassy and rubbery polymers, that the value of the diffusion coefficient for a solvent molecule in a polymeric material changes by orders of magnitude in a narrow concentration interval as the material undergoes its glass transition. This fact has been recognized by a number of authors in the past.[7,15,69] We will now show that a simple description of the diffusion process which properly accounts for these different values and which is otherwise based only on Fick's law is sufficient to reproduce the three features identified above.

The measurements described in the Experimental Section show that the glass transition temperature, T_g, is a function of the methanol volume fraction within EVOH (see Figure 5): The inverse relation defines at each temperature a "critical" solvent volume fraction, $\tilde{\phi}(T)$, above which plasticization occurs. At each given temperature T, there should be a relatively small ϕ range around $\tilde{\phi}(T)$ where the (mutual) diffusion coefficient, $D(\phi)$, jumps abruptly from a very low value, D_0, characteristic of the glassy phase to a high value, D_1, characteristic of the rubbery phase. A "Fermi function" form:

$$D(\phi) = D_0 + \frac{D_1 - D_0}{1 + e^{-L(\phi - \tilde{\phi})}} \tag{1}$$

for the diffusion coefficient reproduces these features.[70] The parameter L controls the size of the transition region around $\tilde{\phi}$. Equation 1 describes the ϕ dependence of the diffusion coefficient at a given temperature. Since $\tilde{\phi}(T)$ is the inverse of $T_g(\phi)$ (see Figure 5), eq 1 implies that when the temperature of the experiment is raised (lowered) the solvent level ϕ at which $D(\phi)$ changes from D_0 to D_1 is itself lowered (raised). In other words a change in T has the effect of translating the "Fermi function" $D(\phi)$ along the ϕ axis. It should be stressed that in this framework $\tilde{\phi}(T)$ provides the connection between the diffusion process and solvent-induced changes in T_g.

We computed the solvent concentration profiles and the sorption and desorption curves predicted for diffusion taking place according to Fick's law with several diffusion coefficients of the form (1): In this way the space of the parameters D_0, D_1, $\tilde{\phi}$, and L was explored. Instead of the ordinary diffusion equation, we used the methods described in ref 30; they have the advantage of properly accounting for displacement of polymer as solvent is absorbed. The equations of ref 30 refer to a model situation where the densities of polymer and solvent are the same. As a result, concentrations and volume fractions coincide. Under these assumptions the time evolution of the solvent concentration, $\phi(x_0,t)$, in the volume element of polymer which was located in $x = x_0$ at time $t = 0$ (x_0 is a Lagrangian coordinate) is described by:

$$\frac{\partial \phi(x_0,t)}{\partial t} = (1 - \phi(x_0,t))^2 \left(D(\phi) \frac{\partial^2 \phi(x_0,t)}{\partial x_0^2} + \frac{\partial D(\phi)}{\partial \phi} \left(\frac{\partial \phi(x_0,t)}{\partial x_0} \right)^2 \right) \tag{2}$$

At time t this volume element is displaced to $x = x_R$, where:

$$x_R(x_0,t) = \int_0^{x_0} \frac{dx_0}{1 - \phi(x_0,t)} \tag{3}$$

The concentration profiles can be obtained by solving eq 2 numerically and transforming back to the laboratory frame using eq 3. In practice, significant qualitative differences between the solutions of equations which account for polymer displacement as solvent moves in and those of the ordinary diffusion equation occur only if the final equilibrium volume fraction, ϕ_{eq}, is large. For the MeOH−EVOH system, $\phi_{eq} < 0.3$ in the temperature range that we considered; as a result, qualitative conclusions similar to those reached below can in fact be obtained from the ordinary diffusion equation.

The boundary conditions that we use for a film that initially occupies the domain $|x_0| \le a$ (here $2a$ is the initial film thickness) are for sorption $\phi(|x_0| < a, t = 0) = 0$ and $\phi(x_0 = \pm a, t \ge 0) = \phi_{eq}$ and for desorption $\phi(|x_0| < a, t = 0) = \phi_{eq}$ and $\phi(x_0 = \pm a, t \ge 0) = 0$. Here ϕ_{eq} is the final equilibrium volume fraction of solvent within the polymer-occupied region. These boundary conditions imply that equilibrium is reached at the boundary of the polymer-occupied region as soon as the polymer is put in contact with the solvent; we will see that this assumption has to be modified in order to account for the constraint release effects described above.

The ordinary diffusion equation with a diffusion coefficient which jumps discontinuously from D_0 to D_1 at a given concentration, $\tilde{\phi}$, has been studied in detail by Crank.[71] The problem can be solved analytically for a semi-infinite geometry. At the point $x = X(t)$, where $\phi = \tilde{\phi}$, the concentration is continuous, but there is a

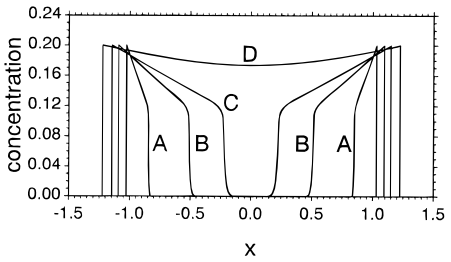

Figure 12. Calculated concentration profiles of penetrant in a slab initially located in $-1 \le x \le 1$ for $D_0 = 0.01$, $D_1 = 1$, $L = 200$, $\tilde{\phi} = 0.12$, and $\phi_{eq} = 0.2$ at times $t = 0.025$ (A), 0.25 (B), 0.63 (C), and 1.58 (D).

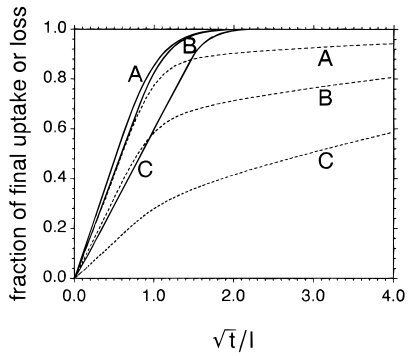

Figure 13. Predicted fractional weight gain (continuous curves) and loss (broken curves) as a function of $\sqrt{t}$ for a film (slab) geometry. Here we used $D_0 = 0.01$, $D_1 = 1$, $\phi_{eq} = 0.2$, and $L = 400$. Different curves correspond to different values of $\tilde{\phi}$: $\tilde{\phi} = 0.03$ (A), 0.08 (B), and 0.15 (C).

discontinuity in the concentration gradient to ensure continuity of the flux. For sorption boundary conditions, namely, $\phi = \phi_{eq}(>\tilde{\phi})$ at the boundary of the semi-infinite domain, the distance of $X(t)$ from the boundary grows like $\sqrt{t}$. In the limit $D_0 \to 0$, the concentration profile itself becomes discontinuous at $x = X(t)$; it drops from $\phi = \tilde{\phi}$ to whatever value ($<\tilde{\phi}$) ϕ initially had within the domain.

Our numerical treatment of eqs 2 and 3 yields similar behavior.[72] For $D_0 < D_1$ by a couple of orders of magnitude and sufficiently large values of L, there are sharp drops in the concentration profiles[73] at the point where $\phi = \tilde{\phi}$. Figure 12 shows examples of solvent concentration profiles within a film at different times during sorption: Here $D_1 = 1$, $D_0 = 0.01$, $\tilde{\phi} = 0.12$, $\phi_{eq} = 0.2$, and $L = 200$. Both the solvent uptake and the distance of the front from the boundary grow like $\sqrt{t}$ at small t. Due to swelling, the film boundaries are moving to larger values of $|x|$ in Figure 12. Ahead of the advancing front there is a low concentration of solvent ("precursor tail"[74]) whose properties are controlled by $D(\phi < \tilde{\phi})$, *i.e.*, essentially by the value D_0 of the diffusion coefficient for the glassy region.

The shape of the sorption curves is affected very little by the value of $\tilde{\phi}$ and (for the same D_0, D_1, and $\tilde{\phi}$) is nearly unchanged by changes in L (as long as L is not so small as to completely smooth out the transition between D_0 and D_1). The time required to reach equilibrium increases as $\tilde{\phi}$ approaches ϕ_{eq}. If D_0 is much smaller than D_1, the flux attributable to diffusion taking place at volume fractions lower than $\tilde{\phi}$ is also very small; as a result, the sorption curves are not sensitive to the actual value of D_0. A sample of sorption curves obtained for $D_0/D_1 = 0.01$, $\phi_{eq} = 0.2$, $L = 400$, and different values of $\tilde{\phi}$ is shown in Figure 13.

While (for $D_1 \gg D_0$) sorption is controlled mainly by D_1, the desorption curves provide information as to the values of D_0 and of $\tilde{\phi}(T)$ at the temperature T of the experiment. Indeed, if the solvent level at which desorption starts is larger than $\tilde{\phi}$, the loss curve exhibits two different regimes. Initially loss proceeds rapidly at a rate controlled by D_1 until the concentration within the sample becomes close to $\tilde{\phi}$. At this stage the rate of solvent loss is drastically reduced since transport of solvent within the sample is now controlled by D_0: the smaller D_0 the slower the desorption. The two regimes are clearly identifiable in the broken lines of Figure 13 which refer to $D_0/D_1 = 0.01$, $\phi_{eq} = 0.2$, $L = 400$, and different values of $\tilde{\phi}$. The crossover between the two desorption regimes takes place in correspondence to $\tilde{\phi}$. In fact, for D_0 strictly equal to zero, the concentration within the sample cannot fall below $\tilde{\phi}$, and the desorption curve becomes flat at large times.

Since the value of $\tilde{\phi}$ is controlled by the temperature T of the experiment, the different desorption curves of Figure 13 are the predictions of our simple description for desorption at different temperatures. In particular, raising the temperature lowers $\tilde{\phi}$; therefore, if the temperature is raised after the slow regime has been reached, the desorption curve will jump to a new slow regime corresponding to the new higher temperature, *e.g.*, to a lower $\tilde{\phi}$. For example, with the parameters used in Figure 13, if T is increased in such a way that $\tilde{\phi}$ changes from 0.08 to 0.03 (and if D_0 remains constant), the desorption curve jumps from curve B to curve A. This is the kind of behavior exhibited by the data reported in Figure 11.

In view of all this, it should be apparent that our numerical results reproduce the three qualitative experimental features listed at the beginning of this section. They are consistent with uptake $\sim \sqrt{t}$ at $t \to 0$ and with a sharp drop in the concentration front at the interface between glassy and plasticized regions. The onset of slow desorption in the data reported in Figures 10 and 11 is also in agreement with our description. For example, on the basis of the data of Figure 5, the onset of slow desorption for F101 should occur at $c_t \approx 0.03-0.04$ for $T = 40$ °C and 0.05−0.06 for $T = 20$ °C (here $c_t = (w_t - w_i)/w_t$), and the desorption data of Figure 10 are consistent with these expectations. Above T_g only the fast regime is present; this is the situation corresponding to the $T = 90$ °C data in Figure 10.

The simple framework put forward thus far does not attempt to account for elastic forces arising between regions of the specimen which in the course of the diffusion process find themselves swollen to different extents. Because of this, it cannot reproduce the sigmoidal shape of the sorption curves and the fact that at $t \to 0$ desorption is faster than sorption. In order to explain these results, we have to examine the constraints which the plasticized region experiences during the sorption process due to the presence of the glassy core.

In particular, the results of refs 35 and 36 for the equilibrium swelling of rubber adhesively bonded to a rigid substrate show the following. (i) For a film or slab, as long as the constraint is active, the maximum value (neglecting edge effects) of the solvent volume fraction within the plasticized region is equal to $\phi_{eq}^{(1)}$; $\phi_{eq}^{(1)}$ is the equilibrium volume fraction for a thin layer of rubber bonded to a spherical core whose radius tends to infinity and can be estimated solving the one-dimensional Flory−Rehner[75,76] problem. When the constraint is

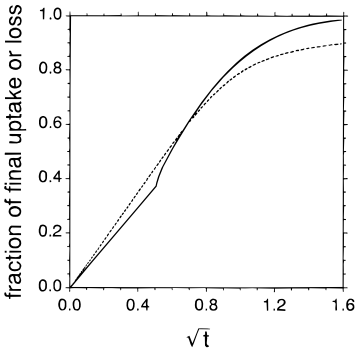

Figure 14. Fractional weight gain (continuous curves) and loss (broken curves) as a function of $\sqrt{t}$ for a film (slab) geometry predicted taking into account the effect of constraint release during the sorption process. Here we used $D_0 = 0.001$, $D_1 = 1$, $\phi_{eq}^{(1)} = 0.16$, $\phi_{eq}^{(3)} = 0.2$, $\tilde{\phi} = 0.03$, and $L = 400$.

released, *e.g.*, when the central layer is finally plasticized, the solvent volume fraction can grow to its final equilibrium value, $\phi_{eq}^{(3)}$ ($=\phi_{eq}$), found from the solution of the three-dimensional Flory−Rehner problem. (ii) For a cylinder, as the core gets thinner and thinner, the maximum value of the solvent volume fraction (at the solvent−polymer boundary) grows gradually from $\phi_{eq}^{(1)}$ to $\phi_{eq}^{(2)}$ (the solution of the two-dimensional problem). Again, it is only when the constraint is released that the solvent volume fraction can increase to the final value $\phi_{eq}^{(3)}$. (iii) For a sphere the volume fraction at the outer sample boundary simply grows gradually from $\phi_{eq}^{(1)}$ to $\phi_{eq}^{(3)}$ as the size of the glassy core gets smaller. It is worth noting that the naive picture of Figure 2 essentially captures this behavior.

The equilibrium volume fraction $\phi_{eq}^{(3)}$ is larger than the value $\phi_{eq}^{(1)}$ of the solvent volume fraction at the boundary when the sorption process begins, and both these quantities are independent of sample geometry.[77] Therefore, if the diffusion coefficient is the same, the flux (out) at the initial stages of desorption is larger than the flux (in) at the initial stages of sorption. In fact, in view of the measured value of $\phi_{eq}^{(3)}$ in our system, it is easy to see that for a large class of reasonable free energies $\phi_{eq}^{(3)}$ exceeds $\phi_{eq}^{(1)}$ by ≈25% and that the value of $\phi_{eq}^{(2)}$ is only a few percent lower than that of $\phi_{eq}^{(3)}$. Furthermore, the area of the swollen sample is also larger, a fact which is crucial in giving faster desorption than sorption in the system of ref 29. The calculations outlined below show that these two effects can lead to desorption faster than sorption at $t \to 0$.

In order to obtain an estimate for the effect of constraint release on the shape of the sorption curve for a film or slab, we solve the problem of eqs 1−3 using $\phi(x_0 = \pm a, t > 0) = \phi_{eq}^{(1)}$ as the initial boundary condition. However, at the time $\tilde{t}$ when the solvent volume fraction at the center of the slab $\phi(x_0 = 0,t)$ exceeds $\tilde{\phi}$, *e.g.*, when the constraint from the central glassy layer is finally released, we change the boundary conditions to $\phi(x_0 = \pm a, t > \tilde{t}) = \phi_{eq}^{(3)}$. The continuous curve of Figure 14 shows an example of the results that we obtain through this procedure: The regime of accelerated uptake appears as a sudden change in the slope of the computed sorption curve. The parameters used to obtain these results were chosen in a range which approximately matches[78] our system at 40 °C. However, the qualitative prediction of an accelerated uptake is largely independent of the value of the parameters: As $\tilde{\phi}$ increases, accelerated uptake begins at later times since it takes longer for the central region to become plasticized. While our estimate for the sorption curve does not try to describe in detail the three-dimensional rearrangement which takes place when the constraint is released, it captures its effect in an indirect way.[79] In practice, constraint release is not going to be as sudden as in our model problem (as shown in Figure 4, the change in modulus at the glass transition is a gradual process); therefore it is not surprising that the transition to accelerated uptake is smoother in our experimental data that in the computed sorption curve of Figure 14.

Figure 14 also shows the desorption curve obtained solving the problem of eqs 1−3 using as boundary conditions $\phi(|x_0| < a, t = 0) = \phi_{eq}^{(3)}$ and $\phi(x_0 = \pm a, t \geq 0) = 0$. At $t \to 0$, desorption is faster than sorption, even though the effect of the area increase in the swollen sample (which makes desorption even faster) is neglected in this estimate. We found (again neglecting the area effect), that, as $\tilde{\phi}$ increases, the initial slopes of the sorption and desorption curves become closer until, above a certain threshold, sorption becomes faster.[80] We note that macroscopic elastic stresses within the sample also arise during desorption; in particular, in the desorption process the outer (solvent-depleted) regions are subject to tensile stresses from the still swollen core. However, the procedure used here to obtain the desorption curve of Figure 14 neglects these effects.

In order to obtain estimates for the geometry dependent effects in the case of the cylinder and the sphere, we proceed as follows. First, we choose values of χ and N (here N is the effective number of monomers between cross-links) in the Flory−Rehner problem which produce a realistic value for $\phi_{eq}^{(3)}$. We then solve (for these χ and N) the equilibrium-constrained swelling problem for the cylinder[35] and the sphere[36] using different values of the ratio ρ between the radius of the rigid core and the (unswollen) outer radius of the rubber tube or shell.[81] In this way, we obtain the value ϕ_b of the equilibrium solvent volume fraction at the outer (solvent−polymer) boundary as a function of ρ.

The kinetic sorption problems that we solve are the two- and three-dimensional analogs of the problem of eqs 2 and 3 with a mutual diffusion coefficient having the form given in eq 1 (the reader is referred to refs 29 and 30 for details on the form of these equations). Again we account for movement of the polymer as solvent moves in (or out). The data for ϕ_b as a function of ρ obtained from the solution of the equilibrium-constrained swelling problem are used as boundary conditions in the corresponding kinetic problem. For example, in the cylinder case, we use as initial boundary condition $\phi(r_0 = a, t = 0) = \phi_b(\rho = 1)$. However, as the radius of the glassy core becomes smaller, we change this boundary condition to the appropriate value of ϕ_b, *e.g.*, $\phi(r_0 = a, t(\rho)) = \phi_b(\rho)$, where $t(\rho)$ denotes the time at which the radius of the core is equal to a fraction, ρ, of the initial radius. When eventually the solvent volume fraction at the center of the cylinder exceeds $\tilde{\phi}$, we change the volume fraction at the boundary from $\phi_{eq}^{(2)}$ to $\phi_{eq}^{(3)}$; this is the point where the constraint from the core is finally released.

An example of the results of this procedure is shown in Figure 15. The inset gives our results for ϕ_b as a function of ρ. The discontinuity in the slope of the sorption curve at intermediate times results from changing the volume fraction at the boundary from

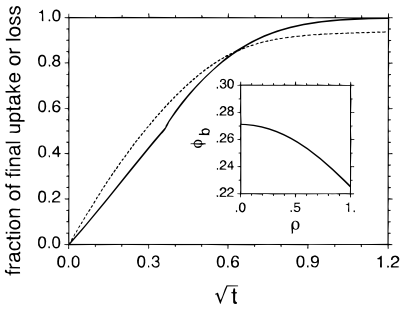

Figure 15. Fractional weight gain (continuous curves) and loss (broken curves) as a function of $\sqrt{t}$ for a cylindrical geometry predicted taking into account the effect of constraint release during the sorption process. Here we used $D_0 = 0.001$, $D_1 = 1$, $\chi = 0.3$, $N = 2.4$, $\phi = 0.03$, and $L = 400$. The inset gives ϕ_b as a function of ρ computed solving the equilibrium-constrained swelling problem. When the volume fraction at the center of the cylinder exceeds $\tilde{\phi}$, the value of the solvent volume fraction at the boundary is changed from $\phi_{eq}^{(2)} = 0.2712$ to $\phi_{eq}^{(3)} = 0.2927$.

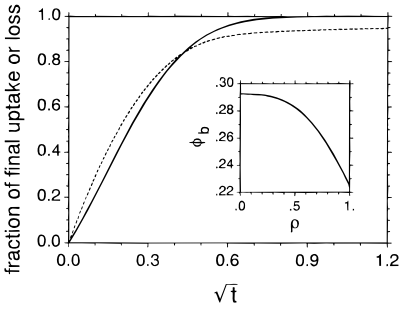

Figure 16. Fractional weight gain (continuous curves) and loss (broken curves) as a function of $\sqrt{t}$ for a spherical geometry predicted taking into account the effect of constraint release during the sorption process. Here we used $D_0 = 0.001$, $D_1 = 1$, $\chi = 0.3$, $N = 2.4$, $\phi = 0.03$, and $L = 400$. The inset gives ϕ_b as a function of ρ computed solving the equilibrium-constrained swelling problem.

$\phi_{eq}^{(2)}$ to $\phi_{eq}^{(3)}$. It marks the onset of an accelerated uptake regime following the final constraint release: The effect is much milder than in the case of the film (Figure 14) because $\phi_{eq}^{(2)}$ is much closer to $\phi_{eq}^{(3)}$ than $\phi_{eq}^{(1)}$. In the case of the sphere (see Figure 16) where constraint release is gradual and ϕ_b interpolates smoothly from $\phi_{eq}^{(1)}$ to $\phi_{eq}^{(3)}$, there is no regime of accelerated uptake. For both the cylinder and the sphere, the sorption curves are concave at very short times. This effect is noticeable but rather small in Figures 15 and 16 because in these examples the final solvent volume fraction is relatively small (the parameters chosen to obtain these figures fall in the range corresponding to our experimental results of Figures 8 and 9). However, the effect is real and becomes more obvious for larger values of the equilibrium solvent volume fraction; it is due to the relatively rapid change in ϕ_b for ρ close to 1. Because of this it is larger in the case of the sphere than in the case of the cylinder (see the insets in Figures 15 and 16). It is tempting to associate this prediction to our observation that a straight line drawn through the $\sqrt{t}$ portion of the sorption data of Figure 9 does not intercept the origin. However, in order to conclusively confirm this conjecture, further experimental work, possibly with a system where ϕ_{eq} is larger, is required.

Figures 15 and 16 also show our results for the desorption curves. The initial concentration within the specimen was taken to be uniform and equal to $\phi_{eq}^{(3)}$; at the boundary ϕ was held to zero throughout the desorption process. Again no attempt was made to account for macroscopic elastic effects during desorption. In both the cylinder and the sphere initially desorption is faster than sorption. Since we account for movement of the polymer as solvent moves in or out, our calculation for the sphere fully accounts for the "area" effect discussed above.

These results show that the constraint release mechanism associated with plasticization provides a rationale for the seemingly disparate "anomalous" features exhibited by our sorption and desorption curves. It accounts for the qualitative differences between the regimes of accelerated uptake found in films and cylinders, for the absence of an accelerated uptake regime late in the sorption process in the case of spheres, and for the fact that desorption is faster than sorption at $t \rightarrow 0$. Our predictions are not based on such *ad hoc* assumptions as complicated dependences of the diffusion coefficient on the state of stress and the history of the sample; instead they are rooted in the physics of the plasticization process.

In spite of all the areas of agreement listed above, it is clear that in order to obtain quantitative predictions a number of other effects, which have been neglected here, must be accounted for. In particular, to avoid obtaining a discontinuous slope for the sorption curves, a more realistic way to treat macroscopic elastic stresses arising during the sorption process is necessary. This also implies accounting for the three-dimensional rearrangement taking place in the film as the constraint from the glassy core is released. Furthermore, the experimental data for desorption appear to indicate that desorption is at $t \rightarrow 0$ even faster than our calculations suggest and that the onset of the slow-desorption regime for spheres and cylinders occurs somewhat sooner than predicted. Again it is likely that a treatment of the macroscopic elastic stresses arising during desorption (which are neglected in our estimates) is required to reproduce these features.

It must be noted in this regard that a general theoretical framework to describe solvent transport coupled to macroscopic elastic effects is at present lacking.[30] The reason we are able to investigate in detail the effects of the constraint release mechanism in the present problem is that we study the limiting situation where a perfectly rigid core is present. As soon as a finite (rather than infinite) modulus is assigned to the core, the problem becomes considerably more complex. A consequence of this is that experiments, such as ours, where a sharp front is present, are, contrary to a commonly held belief, easier to analyze and interpret than the results of differential sorption experiments. In the latter case, in order to deconvolute the constraint release effects out of the sorption data, one cannot avoid treating the full elastic problem.

As noted in the Introduction, complex constitutive relations for the flux different from Fick's law have been used in the past in attempts to account for data of the kind presented in this paper. Our results suggest that a much simpler explanation may be at hand for these and similar "anomalous" results reported in the literature for a number of other systems[17−22] which exhibit initial uptake proportional to $\sqrt{t}$. No modification of Fick's law is required, but both the concentration dependence of the diffusion coefficient and its relation to the plasticization process as well as the geometry dependent macroscopic elastic stresses arising as sol-

vent moves in (or out) of the sample must be properly accounted for. These same physical processes are present and play a role in systems which exhibit true case II behavior, namely, sharp fronts moving at constant velocity and initial uptake linear in time. As we noted in the Introduction, it is possible that, if the kinetics of plasticization are properly accounted for, Fick's law may provide an adequate description of solvent transport even for these systems.

It is not inconceivable, that constraint release may in some instances produce sorption overshoots of the kind shown in Figure 1c.[82] For example, consider a slab in a limiting situation where the central glassy layer remains very rigid until the solvent volume fraction within the layer exceeds $\tilde{\phi}$ but is then very suddenly softened. In this situation, two processes take place. Solvent is taken up by the sample in order to bring the sample area to its equilibrium value, but at the same time the thickness (which before constraint release is much larger than its equilibrium value) must decrease, and this could imply desorption of solvent which had already been taken up. If this second process is slower than the first, it may be possible for sorption overshoots to occur.

In conclusion, we have analyzed the behavior of methanol in EVOH using a combination of dynamic mechanical techniques and sorption and desorption measurements. The results of these two sets of experiments can be related to each other within a simple theoretical description whose ingredients are Fick's law with a diffusion coefficient which reflects the change in state of the material as it undergoes plasticization and a detailed analysis of the macroscopic elastic stresses which arise as a result of the plasticization process. Our description emphasizes the need to distinguish between experimental results which are due to microscopic (material) properties of the system and results which are due to the particular geometry of the sample. Within our framework, a consistent picture can be provided for both the material dependent features of our observations and the geometry dependent effects. We expect that these ideas and methods may prove generally useful in the analysis of the process of solvent diffusion in glassy polymers.

Acknowledgment. We are grateful to David Kubinski, George Lavoie, and Mark Nulman for useful conversations and to Ed Blais, Mo Cheung, and Joe Cassatta for helpful suggestions regarding the experimental setup. We also wish to thank Prof. Phil Pincus for several useful discussions and for a critical reading of the manuscript.

References and Notes

(1) Ferry, J. D. *Viscoelastic properties of polymers*; Wiley: New York, 1980.
(2) An example of such a material is discussed in: Morisato, A.; Miranda, N. R.; Freeman, B. D.; Hopfenberg, H. B.; Costa, G.; Grosso, A.; Russo, S. *J. Appl. Polym. Sci.* **1993**, *49*, 2065.
(3) Stannett, V. In *Diffusion in Polymers*; Crank, J., Park, G. S., Eds.; Academic Press: New York, 1968; p 41.
(4) Pauly, S. In *Polymer Handbook*; Brandrup, J., Immergut, E. H., Eds.; Wiley: New York, 1989; p VI/435.
(5) Meares, P. *J. Am. Chem. Soc.* **1954**, *76*, 3415. Meares, P. *Trans. Faraday Soc.* **1957**, *53*, 101.
(6) The final uptake can be small either due to the very low affinity between solvent and polymer molecules (as in the systems of ref 5) or due to the very low activity to which the polymer is intentionally exposed.
(7) At least two examples of systems where substantial (over 10%) solvent uptake is not sufficient to lower the nominal T_g of the soaked polymer below the temperature of the experiment have actually been reported. These are methanol diffusing in PMMA below 15 °C and *n*-hexane in PPO; see: Thomas, N. L.; Windle, A. H. *Polymer* **1980**, *21*, 613. Jacques, C. H. M.; Hopfenberg, H. B.; Stannett, V. *Polym. Eng. Sci.* **1973**, *13*, 81. Jacques, C. H. M.; Hopfenberg, H. B. *Polym. Eng. Sci.* **1974**, *14*, 441, 449.
(8) In these systems the diffusion coefficient is usually taken to be independent of concentration (which at any rate is very small).
(9) Alfrey, T.; Gurnee, E. F.; Lloyd, W. G. *J. Polym. Sci., Part C* **1966**, *12*, 249.
(10) Kwei, T. K.; Zupko, H. M. *J. Polym. Sci., Part A-2* **1969**, *7*, 867.
(11) Michaels, A. S.; Bixler, H. J.; Hopfenberg, H. B. *J. Appl. Polym. Sci.* **1968**, *12*, 991. Hopfenberg, H. B.; Holley, R. H.; Stannett, V. *Polym. Eng. Sci.* **1969**, *9*, 242. Holley, R. H.; Hopfenberg, H. B.; Stannett, V. *Polym. Eng. Sci.* **1970**, *10*, 376. Nicolais, L.; Drioli, E.; Hopfenberg, H. B.; Tidone, D. *Polymer* **1977**, *18*, 1137.
(12) Andrews, E. H.; Levy, G. M.; Willis, J. *J. Mater. Sci.* **1973**, *8*, 1000. Hopfenberg, H. B.; Nicolais, L.; Drioli, E. *Polymer* **1976**, *17*, 195. Nicolais, L.; Drioli, E.; Hopfenberg, H. B.; Caricati, G. *J. Membr. Sci.* **1978**, *3*, 231.
(13) Thomas, N. L.; Windle, A. H. *Polymer* **1977**, *18*, 1195. Thomas, N. L.; Windle, A. H. *Polymer* **1978**, *19*, 255. Thomas, N. L.; Windle, A. H. *Polymer* **1981**, *22*, 627.
(14) Mills, P. J.; Palmstrøm, C. J.; Kramer, E. J. *J. Mater. Sci.* **1986**, *21*, 1479.
(15) Hui, C. Y.; Wu, K. C.; Lasky, R. C.; Kramer, E. J. *J. Appl. Phys.* **1987**, *61*, 5129, 5137. Lasky, R. C.; Kramer, E. J.; Hui, C. Y. *Polymer* **1988**, *29*, 673.
(16) Gall, T. P.; Kramer, E. J. *Polymer* **1991**, *32*, 265.
(17) Crank, J.; Park, G. S. *Trans. Faraday Soc.* **1949**, *45*, 240.
(18) Kokes, R. J.; Long, F. A.; Hoard, J. L. *J. Chem. Phys.* **1952**, *20*, 1711.
(19) Crank, J. *J. Polym. Sci.* **1953**, *11*, 151.
(20) Long, F. A.; Kokes, R. J. *J. Am. Chem. Soc.* **1953**, *75*, 2232.
(21) Long, F. A.; Thompson, L. J. *J. Polym. Sci.* **1955**, *15*, 413. Kishimoto, A.; Fujita, H. *Kolloid Z.* **1957**, *150*, 24.
(22) Billovits, G. D.; Durning, C. J. *Polymer* **1988**, *29*, 1468.
(23) For a review of early techniques, see: Crank, J.; Park, G. S. In *Diffusion in Polymers*; Crank, J., Park, G. S., Eds.; Academic Press: New York, 1968; p 1.
(24) Richman, D.; Long, F. A. *J. Am. Chem. Soc.* **1960**, *82*, 509.
(25) Klein, J.; Briscoe, B. J. *Proc. R. Soc. London* **1979**, *A365*, 53.
(26) Romanelli, J. F.; Mayer, J. W.; Kramer, E. J.; Russel, T. P. *J. Polym. Sci., Polym. Phys. Ed.* **1986**, *24*, 263.
(27) Fujita, H. *Fortschr. Hochpolym. Forsch.* **1961**, *3*, 1.
(28) Including chemical reactions (chain scission, cross-linking), morphological changes (such as solvent-induced crystallization), and possible loss of either trapped solvent used in sample preparation or un-cross-linked polymeric components.
(29) Mazich, K. A.; Rossi, G.; Smith, C. A. *Macromolecules* **1992**, *25*, 6929.
(30) Rossi, G.; Mazich, K. A. *Phys. Rev.* **1991**, *A44*, R4793. Rossi, G.; Mazich, K. A. *Phys. Rev.* **1993**, *E48*, 1182.
(31) Rather than unphysically assuming, as is often done, that the boundary of the polymer-occupied region remains fixed as solvent diffuses into the polymer.
(32) Kwei, T. K. *J. Polym. Sci., Part A2* **1972**, *10*, 1849.
(33) Long, F. A.; Richman, D. *J. Am. Chem. Soc.* **1960**, *82*, 513.
(34) It is in this respect different from many common physical phenomena: For example, a one-dimensional description gives a good approximation of the electric field near the surface of a large uniformly charged slab, and the one-dimensional diffusion equation describes well the diffusion of a liquid into a porous (nonswelling) film. In both instances the only corrections to the one-dimensional description come from edge effects.
(35) Treloar, L. R. G. *Polymer* **1976**, *17*, 142.
(36) Mazich, K. A.; Rossi, G. *Macromolecules* **1991**, *24*, 5470. See also: Sternstein, S. S. *J. Macromol. Sci.* **1972**, *B6*, 243.
(37) In certain systems where case II diffusion is observed (see ref 13), the interface between the glassy and plasticized regions moves so slowly that within the plasticized region the concentration profile is nearly constant and presumably close to the equilibrium concentration profile predicted in Treloar's problem. In these systems both the final solvent concentration, $c^{(eq)}$, and the solvent concentration when the constraint from the rigid inner layer is still active, $c^{(constr)}$, can be measured (the latter from maximum thickness increase in the sample). The authors of ref 13 use these data to determine χ and N (here N is the effective number of monomers between cross-links). However, the form of the

free energy is subject to large uncertainty, so one should probably be content with checking that sensible results for $c^{(eq)}$ and $c^{(constr)}$ are obtained independently of the detailed form of the free energy. For example, using Treloar's form with $\chi = 0.65$ and $N = 4$, one gets $c^{(eq)} = 0.275$ and $c^{(constr)} = 0.227$, in reasonable agreement with the experimental data.

(38) These are the forces responsible for the crazing and fracture behavior reported in a number of such systems; see, for example, refs 9−11.

(39) There is a simple topological reason for this result. In two or three dimensions it is impossible to affinely (uniformly) swell (by a ratio other than 1) the outer rubber tube or shell in Treloar's problem without violating the adjacency constraint at the interface between the rigid core and the inner surface of the tube or shell. To satisfy this constraint (which is forced upon the problem by the requirement of adhesive bonding), elastic stresses and concentration gradients must arise. On the other hand, in one dimension the adjacency constraint can be satisfied for any affine deformation.

(40) Over the years several authors have attempted to account for the effect of swelling within a one-dimensional description, *e.g.*, using only the component of the stress perpendicular to the film surface (which for a film is essentially zero as noted in the text). A recent example is found in: Wu, J. C.; Peppas, N. A. *J. Polym. Sci., Part B* **1993**, *31*, 1503.

(41) Firestone, B. A.; Siegel, R. A. *Polym. Commun.* **1988**, *29*, 204. See also: Siegel, R. A. *Adv. Polym. Sci.* **1993**, *109*, 233. These authors provide experimental evidence on how the thickness of their gels affects the onset of the regime of accelerated uptake.

(42) A version of the mechanism described here also has been invoked in ref 13 to account for the so-called "super case II" behavior, *e.g.*, sorption curves displaying uptake growing like t^{α} with $\alpha > 1$ late in the sorption process.

(43) Other treatments which attempt to deal with macroscopic elastic forces arising in the sample in the course of the diffusion process have been proposed. In addition to refs 9 and 19, see: Rosen, B. *J. Polym. Sci.* **1961**, *19*, 177. Petropoulos, J. H.; Roussis, P. P. *J. Membr. Sci.* **1978**, *3*, 343. Petropoulos, J. H. *J. Polym. Sci.* **1984**, *22*, 183. Gostoli, C.; Sarti, G. C. *Polym. Eng. Sci.* **1982**, *22*, 1018.

(44) Billovits, G. F.; Durning, C. J. *Macromolecules* **1993**, *26*, 6927.

(45) Fujita, H. In *Diffusion in Polymers*; Crank, J., Park, G. S., Eds.; Academic Press: New York, 1968; p 75.

(46) Astarita, G.; Sarti, G. C. *Polym. Eng. Sci.* **1978**, *18*, 388.

(47) Rossi, G.; Pincus, P. A.; de Gennes, P. G. *Europhys. Lett.* **1995**, *32*, 391.

(48) Actually the term "swelling" is used in ref 46 to denote the undoing of the glassy state (*i.e.*, plasticization).

(49) An attempt to deal with a nonzero diffusion coefficient in the glassy region ($D_0 \neq 0$) is found in: Astarita, G.; Joshi, S. *J. Membr. Sci.* **1978**, *4*, 165. Within this model the authors present a proof showing that for a certain range of sample sizes the initial uptake is proportional to $\sqrt{t}$ while for other sizes it is linear in t. This result goes against the local nature of the model. Indeed, if at $t \to 0$ the uptake were proportional to $\sqrt{t}$ at the polymer−solvent interface ($x = 0$), one would have $\int_0^t \partial_x\phi(x = 0,t)dt \sim t^{1/2}$ (here $\phi(x,t)$ is the solvent volume fraction). This implies that $\partial_x\phi(x = 0,t) \sim t^{-1/2}$ diverges at $t \to 0$, in contradiction to one of the proof assumptions that $\phi(x,t)$ be constant and equal to the final equilibrium volume fraction in the region between the solvent−polymer and the rubbery−glassy interfaces. In a self-consistent local continuum model (even with $D_0 \neq 0$), the initial uptake should be linear in t and independent of sample size.

(50) Sarti, G. C. *Polymer* **1979**, *20*, 827.

(51) Thomas, N. L.; Windle, A. H. *Polymer* **1982**, *23*, 529.

(52) Vrentas, J. S.; Jarzebski, C. M.; Duda, J. L. *AIChE J.* **1975**, *21*, 894.

(53) Durning, C. J.; Tabor, M. *Macromolecules* **1986**, *19*, 2220.

(54) Adib, F.; Neogi, P. *AIChE J.* **1987**, *33*, 164.

(55) Lustig, S. R.; Peppas, N. A. *J. Appl. Polym. Sci.* **1987**, *33*, 533.

(56) Roda, G. C.; Sarti, G. C. *AIChE J.* **1990**, *36*, 851.

(57) The same kind of argument can be given and the same paradoxical conclusions can be reached in connection with differential sorption experiments.

(58) The treatments leading to these results are flawed in a number of other respects. In particular, the inherently three-dimensional geometrical effects discussed in the present paper are systematically neglected. Furthermore, different physical quantities pertaining to either a macroscopic or a microscopic description are incorrectly blended together. Specifically, there seems to be considerable confusion concerning the nature of osmotic pressure. For a discussion in this regard, see: Denbigh, K. *The Principles of Chemical Equilibrium*; Cambridge University Press: Cambridge, 1981.

(59) We are aware of only one set of experimental results where the initial uptake has been reported to change from linear to $\sqrt{t}$ depending on the size of the sample. Polystyrene spheres exposed to hexane have been reported to exhibit case II behavior if the diameter is $d = 184$ μm and Fickian behavior if $d = 0.534$ μm; see: Enscore, D. J.; Hopfenberg, H. B.; Stannett, V. T. *Polymer* **1977**, *18*, 793. Hopfenberg, H. B. *J. Membr. Sci.* **1978**, *3*, 215. Berens, A. R.; Hopfenberg, H. B. *Polymer* **1978**, *19*, 489. With regard to these results we note the following. The two sets of spheres were prepared via different polymerization processes: suspension polymerization for the large spheres and emulsion polymerization for the small ones. The final uptake for the small spheres is nearly 2 times as large as the final uptake for the large spheres under identical exposure conditions. This points to morphological differences between the two materials. In particular, we note that the presence of micropores in the smaller spheres would account for both the initial Fickian behavior (solvent would simply move into the pores following Darcy's law) and the higher equilibrium uptake. Such a difference in morphology would also account for the reported deviation from Fickian behavior observed at finite times, since diffusion of solvent from the pores into the glassy polystyrene would still be controlled by case II diffusion. No attempt to characterize the spheres from a morphological standpoint is reported in the papers quoted above.

(60) This is true of a number of other models where the Deborah number concept is not explicitly invoked; see: Carbonell, R. G.; Sarti, G. C. *Ind. Eng. Chem. Res.* **1990**, *29*, 1194. Kalospiros, N. S.; Ocone, R.; Astarita, G.; Meldon, J. H. *Ind. Eng. Chem. Res.* **1991**, *30*, 851. Jou, D.; Camacho, J.; Grmela, M. *Macromolecules* **1991**, *24*, 3597.

(61) It is curious in this regard that ref 9 is often misquoted as the work which introduced the concept of "relaxation-controlled transport". In fact, in the paper by Alfrey, Gurnee, and Lloyd, the word "relaxation" appears only once: It is mentioned as an aside, while work by previous authors (who had claimed a role for it) is reviewed.

(62) The plasticized region of the material is similar from a material standpoint to a rubbery polymer. The glassy region is similar to the systems of ref 5. In both instances Fick's law is expected to hold.

(63) Lustig, S. R.; Caruthers, J. M.; Peppas, N. A. *Chem. Eng. Sci.* **1992**, *47*, 3037. Hayes, C. K.; Cohen, D. S. *J. Polym. Sci., Part B* **1992**, *30*, 145.

(64) In the course of each run on the equilibrated material, methanol desorbs from the samples. Significant desorption takes place only after the temperature exceeds T_g (see Discussion). In the worst case, ≈18% of the original methanol was lost. This means that above T_g the value of the storage modulus at the methanol weight fraction measured before the run may be somewhat lower than that reported in Figure 4.

(65) Toyoshima, K. In *Polyvinyl Alcohol*; Finch, C. A., Ed.; Wiley: New York, 1973; p 339.

(66) We obtained similar results for the system water−EVOH in the 25−50 °C temperature range. Results for water sorption in EVOH (for different copolymer compositions from those studied here) have also been reported by: Hopfenberg, H. G.; Apicella, A.; Saleeby, D. E. *J. Membr. Sci.* **1981**, *8*, 273. We disagree with their interpretation of these results in terms of case II diffusion. In particular, we view the apparent linear regime as an artifact due to the pronounced accelerated uptake. Once the data collected by these authors are plotted vs $\sqrt{t}$ (rather than vs t), they all (except for those taken at $T = 0.5$ °C which is very close to the freezing point of water) have the sigmoidal shape shown in our figures and the initial behavior is consistent with $\sqrt{t}$ uptake.

(67) A similar increase in solvent uptake after the fronts have met is also found in case II diffusion. See the data of ref 13 and of Sarti, G. C.; Gostoli, C.; Masoni, S. *J. Membr. Sci.* **1983**, *15*, 181. However, in case II diffusion the effect on weight gain is less dramatic, due to the fact that the concentration of solvent in the plasticized region is nearly flat; in systems such as ours which follow Fick's law, there is a significant gradient (see Figure 12) in the plasticized region. In other words, when the fronts meet, a case II system is much closer to its equilibrium weight uptake than a system of the kind discussed here.

(68) In ref 22, measurements of the front velocity of DMF as it diffuses in PET are reported. The velocity is initially

proportional to $t^{-1/2}$, and the authors describe this behavior as the transport-limited regime of the Astarita−Sarti model, *e.g.*, the behavior is controlled by Fick's law as in our system. However, we disagree with the description given by these authors of sorption of acetone in the same material, which is interpreted as case II diffusion: No data regarding the velocity of the front are given for acetone, and the apparent linear portion in the sorption curves is, in fact, the result of an accelerated uptake regime coincident with the onset of a sudden increase in the transverse dimension of the film. As is the case with the data of ref 67, this effect is immediately apparent once the data are plotted vs $\sqrt{t}$.

(69) Kwei, T. K.; Wang, T. T.; Zupko, H. M. *Macromolecules* **1972**, *5*, 645. Wang, T. T.; Kwei, T. K. *Macromolecules* **1973**, *6*, 919.

(70) In eq 1 D_0 and D_1 are taken to be independent of ϕ, although in reality a (comparatively) mild additional increase of both D_0 and D_1 with ϕ will be present in both the glassy and plasticized phases. Furthermore, in addition to the T dependence of the diffusion coefficient described by eq 1 (through the function $\tilde{\phi}(T)$), one should probably also expect an additional weak T dependence for both D_0 and D_1.

(71) Crank, J. *Trans. Faraday Soc.* **1951**, *47*, 450.

(72) It should be stressed that the general features of our results do not depend on the detailed "Fermi function" form of the diffusion coefficient that we chose to use. Any $D(\phi)$ changing from D_0 to D_1 in a relatively narrow concentration interval whose location reflects the temperature of the experiment in relation to T_g will lead to similar results.

(73) There have been arguments in the literature as to whether it is possible to have sharp concentration fronts in a system without invoking a large difference between D_1 and D_0. We simply view the difference between D_1 and D_0 as an experimental fact.

(74) Note, however, that since our front is not moving at a constant velocity, the precursor tail has the error function form of Crank (see ref 71) and not the (case II) form discussed by: Peterlin, A. *Polym. Lett.* **1965**, *3*, 1083. Peterlin, A. *Makromol. Chem.* **1969**, *124*, 136.

(75) Flory, P. J. *Principles of Polymer Chemistry*; Cornell University Press: Ithaca, NY, 1953.

(76) Treloar, L. R. G. *The Physics of Rubber Elasticity*; Oxford University Press: Oxford, 1975.

(77) The fact that at $t \rightarrow 0$ the solvent volume fraction at the boundary is independent of sample geometry is a manifestation of the fact discussed in the Introduction that at $t \rightarrow 0$ every geometry is effectively semi-infinite; swelling is constrained to the direction normal to the surface, but the effect of these constraints is geometry independent.

(78) Note that the density of methanol is only about two-thirds the density of EVOH. As a result, the volume fraction of solvent is significantly larger than the concentration.

(79) This procedure is similar to that considered in ref 33. However, the way our boundary conditions change reflects the results of the constrained swelling problem for the sample geometry under consideration.

(80) We also verified that the effect of a D_1 which, rather than being constant, increases with ϕ is to move the sorption and desorption curves closer to each other at $t \rightarrow 0$; however, this effect is weak for reasonable forms of $D_1(\phi)$.

(81) For values of χ and N which are reasonable for our system (*i.e.*, that produce equilibrium solvent volume fractions of the order of 0.2−0.3), the equilibrium concentration profiles within the rubber tube or shell are very fast. If this was not the case, the procedure that we adopt to deal with the kinetic problem would not be appropriate, and a potential term (which accounts for the effect of the constraint on the equilibrium profile) would have to be included in the kinetic equations. See the second of ref 30 for details.

(82) In analyzing this type of result, it is important to evaluate the effect of possible morphological changes, such as solvent-induced crystallization (Kambour, R. P.; Karasz, F. E.; Daane, J. H. *J. Polym. Sci., Part A-2* **1967**, *4*, 327. Overbergh, N.; Berghmans, H.; Smets, G. *Polymer* **1975**, *16*, 703) and loss of low molecular weight components (Faulkner, D. L.; Hopfenberg, H. B.; Stannett, V. T. *Polymer* **1977**, *18*, 1130) or uncross-linked chains. We note in this regard that loss of uncross-linked chains (rather than some "relaxational process") may account for the overshoots reported in: Smith, M. J.; Peppas, N. A. *Polymer* **1985**, *26*, 569. Peppas, N. A.; Urdahl, K. G. *Polym. Bull.* **1986**, *16*, 201. No attempt to check for the presence of polymer in solution at the end of the sorption experiment nor any comparison between the initial weight of the sample and a dry final weight (obtained by desorbing the sample after swelling) are reported in these papers.

MA950767P